

LHC HIGGS CROSS SECTION WORKING GROUP  
PUBLIC NOTE

---

Benchmark scenarios for low  $\tan \beta$  in the MSSM

---

Emanuele Bagnaschi<sup>1,a</sup>, Felix Frensch<sup>2,b</sup>, Sven Heinemeyer<sup>3,c</sup>,  
Gabriel Lee<sup>4,d</sup>, Stefan Liebler<sup>1,e</sup>, Margarete Mühlleitner<sup>2,f</sup>, Allison Mc Carn<sup>5,g</sup>,  
Jérémie Quevillon<sup>6,h</sup>, Nikolaos Rompotis<sup>7,i</sup>, Pietro Slavich<sup>8,j</sup>, Michael Spira<sup>9,k</sup>,  
Carlos E.M. Wagner<sup>10,11,l</sup>, and Roger Wolf<sup>2,m</sup>

<sup>1</sup> *Deutsches Elektronen Synchrotron (DESY), Hamburg, Germany*

<sup>2</sup> *Karlsruhe Institut für Technologie (KIT), Karlsruhe, Germany*

<sup>3</sup> *Instituto de Física de Cantabria (CSIC-UC), Santander, Spain*

<sup>4</sup> *Technion-Israel Institute of Technology, Haifa 32000, Israel*

<sup>5</sup> *University of Michigan, Ann Arbor, MI 48109, USA*

<sup>6</sup> *King's College, London, United Kingdom*

<sup>7</sup> *University of Washington, Seattle, WA, USA*

<sup>8</sup> *Laboratoire de Physique Théorique et Hautes Energies (LPTHE), Paris, France*

<sup>9</sup> *Paul Scherrer Institut (PSI), Villigen, Switzerland*

<sup>10</sup> *EFI and KICP, University of Chicago, Chicago, IL 60637, USA*

<sup>11</sup> *HEP Division, Argonne National Laboratory, Argonne, IL 60439, USA*

---

<sup>a</sup>emanuele.bagnaschi@desy.de

<sup>b</sup>felix.frensch@cern.ch

<sup>c</sup>sven.heinemeyer@cern.ch

<sup>d</sup>leeg@physics.technion.ac.il

<sup>e</sup>stefan.liebler@desy.de

<sup>f</sup>margarete.muehlleitner@kit.edu

<sup>g</sup>allison.renae.mc.carn@cern.ch

<sup>h</sup>jeremie.quevillon@kcl.ac.uk

<sup>i</sup>nikolaos.rompotis@cern.ch

<sup>j</sup>slavich@lpthe.jussieu.fr

<sup>k</sup>michael.spira@psi.ch

<sup>l</sup>cwagner@hep.anl.gov

<sup>m</sup>roger.wolf@cern.ch

## Abstract

The run-1 data taken at the LHC in 2011 and 2012 have led to strong constraints on the allowed parameter space of the MSSM. These are imposed by the discovery of an approximately SM-like Higgs boson with a mass of  $125.09 \pm 0.24$  GeV and by the non-observation of SUSY particles or of additional (neutral or charged) Higgs bosons. For low values of the parameter  $\tan \beta$ , the direct bounds on the masses of the additional Higgs bosons are still relatively weak, but very heavy SUSY particles are required to reproduce the observed mass of the SM-like Higgs boson. In this document we discuss and compare two approaches for predicting the properties of the Higgs bosons in the region with low  $\tan \beta$  and heavy SUSY. We also make recommendations for the sets of parameters to be used by the ATLAS and CMS collaborations in the analysis of such scenarios.

# 1 Introduction

In contrast to the SM, the *minimal supersymmetric standard model* (MSSM) requires the introduction of two complex Higgs doublets,  $H_u$  and  $H_d$ , to provide masses for up- and down-type fermions via the spontaneous breaking of the  $SU(2)_L \times U(1)_Y$  gauge symmetry. If the MSSM Lagrangian does not contain new sources of  $CP$  violation, the presence of two complex Higgs doublets implies the existence of two charged Higgs bosons,  $H^\pm$ , and three neutral Higgs bosons: a  $CP$ -odd (i.e., pseudoscalar) state  $A$ , and two  $CP$ -even (i.e., scalar) states,  $h$  and  $H$ , with  $m_h < m_H$ . At the tree level in the MSSM, the masses of these five Higgs bosons and their mixing can be expressed in terms of the gauge-boson masses  $m_W$  and  $m_Z$  plus two additional parameters, which can be chosen as the pseudoscalar mass  $m_A$  and the ratio of the vacuum expectation values of the neutral components of the two Higgs doublets,

$$\tan \beta = \frac{\langle H_u^0 \rangle}{\langle H_d^0 \rangle} = \frac{v_u}{v_d}. \quad (1)$$

The tree-level mass of the charged states is given by  $m_{H^\pm}^2 = m_A^2 + m_W^2$ . The tree-level mass matrix for the neutral  $CP$ -even states reads:

$$\mathcal{M}_{\text{tree}}^2 = \begin{pmatrix} m_A^2 \sin^2 \beta + m_Z^2 \cos^2 \beta & -(m_A^2 + m_Z^2) \sin \beta \cos \beta \\ -(m_A^2 + m_Z^2) \sin \beta \cos \beta & m_A^2 \cos^2 \beta + m_Z^2 \sin^2 \beta \end{pmatrix}. \quad (2)$$

This is diagonalized by an angle  $\alpha$  given by

$$\tan \alpha = \frac{-(m_A^2 + m_Z^2) \sin 2\beta}{(m_Z^2 - m_A^2) \cos 2\beta + \sqrt{(m_A^2 + m_Z^2)^2 - 4m_A^2 m_Z^2 \cos^2 2\beta}}, \quad (3)$$

leading to the tree-level mass eigenvalues

$$m_{h, H}^2 = \frac{1}{2} \left( m_A^2 + m_Z^2 \mp \sqrt{(m_A^2 + m_Z^2)^2 - 4m_A^2 m_Z^2 \cos^2 2\beta} \right). \quad (4)$$

In the MSSM the role of the SM Higgs boson is shared between the scalars  $h$  and  $H$ . In particular, the couplings of the neutral scalars to pairs of massive vector bosons ( $VV$ ) and of SM fermions ( $uu$ ,  $dd$  and  $\ell\ell$ ), relative to the corresponding SM couplings, are:

	$g_{VV}$	$g_{uu}$	$g_{dd, \ell\ell}$
$A$	0	$\cot \beta$	$\tan \beta$
$H$	$\cos(\beta - \alpha)$	$\sin \alpha / \sin \beta$	$\cos \alpha / \cos \beta$
$h$	$\sin(\beta - \alpha)$	$\cos \alpha / \sin \beta$	$-\sin \alpha / \cos \beta$

(5)

In addition, there are non-SM couplings of the neutral scalars to  $Z A$  and to  $W^\pm H^\mp$ . These are proportional to  $\cos(\beta - \alpha)$  in the case of  $h$  and to  $\sin(\beta - \alpha)$  in the case of  $H$ , while the  $Z A A$  coupling vanishes and the  $W^\pm H^\mp A$  coupling does not depend on  $\alpha$  or  $\beta$ . Also relevant for our discussion is the trilinear coupling of one heavy scalar to two light scalars, whose tree-level value reads, in units of  $m_Z^2/v$  where  $v \equiv (v_u^2 + v_d^2)^{1/2} \approx 246$  GeV,

$$\lambda_{Hhh, \text{tree}} = 2 \sin 2\alpha \sin(\beta + \alpha) - \cos 2\alpha \cos(\beta + \alpha). \quad (6)$$

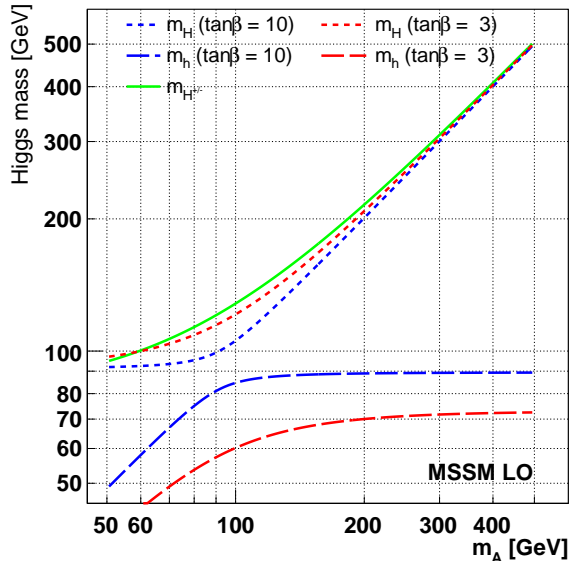


Figure 1: Tree-level values of the masses of the charged scalars,  $m_{H^\pm}$ , and of the neutral scalars,  $m_{H,h}$ , given as a function of the pseudoscalar mass  $m_A$ , for two different values of  $\tan\beta$ .

The tree-level dependence of  $m_H$ ,  $m_h$  and  $m_{H^\pm}$  on  $m_A$ , for two different values of  $\tan\beta$ , is illustrated in Figure 1. In the *decoupling limit*,  $m_A \gg m_Z$ , the mixing angle in the  $CP$ -even sector simplifies to  $\alpha \approx \beta - \pi/2$ . As a result, the tree-level mass of the light neutral scalar  $h$  becomes approximately constant,  $m_h \approx m_Z |\cos 2\beta|$ , and its couplings to gauge bosons, quarks and leptons in Eq. (5) become SM-like. The masses of  $H$  and  $H^\pm$  become approximately degenerate with  $m_A$ , the couplings of  $H$  to two massive gauge bosons vanish, the couplings of  $H$  to two up-type (down-type) SM fermions are suppressed (enhanced) for large  $\tan\beta$ , and the coupling of  $H$  to two light neutral scalars is suppressed for large  $\tan\beta$ . Therefore, in this limit, the Higgs sector of the MSSM reduces to a SM-like Higgs boson with tree-level mass  $m_h < m_Z$ , and a heavy and mass-degenerate multiplet ( $H, A, H^\pm$ ) with vanishing couplings to two massive gauge bosons. In contrast, for low values of  $m_A$  there is a crossing point where  $H$  and  $h$  swap their roles, i.e. the heavy neutral scalar is the one whose mass is independent of  $m_A$  and whose couplings approach SM strength.

Figure 1 shows that, for  $\tan\beta \gtrsim 10$ , the decoupling behavior of the tree-level scalar masses is rather sharp, with a clear crossing point around  $m_A \approx m_Z$ . In contrast, for lower values of  $\tan\beta$  the onset of the decoupling behavior at  $m_A \gg m_Z$  (or  $m_A \ll m_Z$ ) is delayed to larger (or smaller) values of  $m_A$ . Indeed, for  $\tan\beta = 3$  a heavy scalar  $H$  of mass around 300 GeV can still have non-negligible couplings to two massive gauge bosons (as well as to two light scalars, due to the reduced  $\tan\beta$  suppression). However, for low  $\tan\beta$  the upper bound on the tree-level mass of the light scalar can be considerably lower than  $m_Z$ , with  $\tan\beta = 1$  corresponding to a vanishing tree-level mass.

As is well known, the tree-level predictions for the masses of the MSSM Higgs bosons are subject to substantial radiative corrections, which can lift the lightest-scalar mass well above the tree-level bound and introduce a dependence on several other parameters of the MSSM. The dominant one-loop contribution to the lightest-scalar mass arises from loops of top quarks and their scalar superpartners, the top squarks (stops), and in the decoupling limit takes the

approximate form

$$(\Delta m_h^2)_{1\text{loop}}^{t/\bar{t}} \approx \frac{3m_t^4}{2\pi^2 v^2} \left( \log \frac{m_{\text{SUSY}}^2}{m_t^2} + \frac{X_t^2}{m_{\text{SUSY}}^2} - \frac{X_t^4}{12m_{\text{SUSY}}^4} \right), \quad (7)$$

where  $m_{\text{SUSY}} = \sqrt{\overline{m_{\bar{t}_1} m_{\bar{t}_2}}}$  is an average scale for the stop masses, and  $X_t = A_t - \mu \cot \beta$  is the stop mixing term, where  $A_t$  is the soft SUSY-breaking Higgs-stop coupling and  $\mu$  is the higgsino mass parameter. It is easy to see that the one-loop top/stop contribution to  $m_h$  is maximized for large values of  $m_{\text{SUSY}}$  (due to the logarithmic term) and for the *maximal mixing* condition  $|X_t| = \sqrt{6} m_{\text{SUSY}}$ . A smaller negative contribution from sbottom loops, not shown in the equation above, can be relevant only for large values of  $\tan \beta$ . Full one-loop calculations of the MSSM Higgs masses, supplemented with partial two-loop corrections and even the leading three-loop corrections, have become available over the past quarter-century.

The run-1 data taken at the LHC in 2011 and 2012 have led to strong constraints on the allowed parameter space of the MSSM.<sup>1</sup> These constraints are imposed by (i) the discovery of a scalar particle with a mass of  $125.09 \pm 0.24$  GeV [1–3] and couplings compatible with the predictions for the SM Higgs boson within an experimental accuracy of  $\pm(10\text{--}20)\%$  [4, 5]; (ii) the non-observation so far of additional neutral or charged Higgs bosons in direct searches [6–9]; and (iii) the non-observation so far of SUSY particles.

Within the MSSM, the newly discovered particle is usually interpreted as the light neutral scalar  $h$ , while the interpretation as the heavy neutral scalar  $H$  is disfavored by the data [8, 9]. For the set-up and testing of benchmark scenarios, the light-scalar mass is usually treated as a constraint on the unknown SUSY parameters, with the requirement

$$m_h = 125 \pm 3 \text{ GeV}, \quad (8)$$

where the  $\pm 3$  GeV variation corresponds to a rough estimate of the theoretical uncertainty of the MSSM prediction for  $m_h$ , due to the unknown effect of higher-order corrections [10, 11].

For  $\tan \beta \gtrsim 10$  and  $m_A$  in the decoupling region, the tree-level mass of the light scalar saturates the bound  $m_h < m_Z$ ; values of  $m_{\text{SUSY}}$  around one TeV are then necessary to reproduce the observed  $m_h$  in the maximal mixing case, whereas multi-TeV stop masses are necessary for smaller  $|X_t|$ . However, the  $\tan \beta$ -enhancement of the couplings of the heavy Higgs bosons to bottom quarks and to  $\tau$  leptons leads to significant constraints on the  $(m_A, \tan \beta)$  plane from direct searches by ATLAS and CMS [6–9]. For example, the situation in a typical benchmark scenario described in Ref. [12] is shown in Figure 2. In this scenario, values of  $\tan \beta \gtrsim 10$  (20) are directly excluded for  $m_A \lesssim 300$  (500) GeV. For the run-2 LHC the allowed parameter space is expected to shrink further, unless a discovery is made.

For lower values of  $\tan \beta$ , heavy Higgs bosons with masses as low as 200 GeV are not yet excluded by direct searches at the LHC. Moreover, thanks to the delayed approach to the decoupling limit and to the reduced  $\tan \beta$ -suppression of the three-scalar coupling, the decays

$$H \rightarrow WW, \quad H \rightarrow ZZ, \quad H \rightarrow hh, \quad A \rightarrow Zh, \quad (9)$$

may still have significant branching ratios, especially below the threshold for the decay to a top-quark pair (see, e.g., Refs. [13, 14]). However, as mentioned above, lower values of  $\tan \beta$  imply a reduced tree-level mass for the lightest scalar, and hence require larger values of  $m_{\text{SUSY}}$

---

<sup>1</sup>Additional constraints on the MSSM parameter space arise, e.g., from cold dark matter density,  $(g-2)_\mu$  and  $B$ -physics observables. In particular, the latter can exclude regions of the  $(m_A, \tan \beta)$  plane in scenarios where all SUSY contributions decouple. However, such indirect constraints are independent from – and complementary to – those arising from Higgs phenomenology at the LHC, and will not be discussed further in this note.

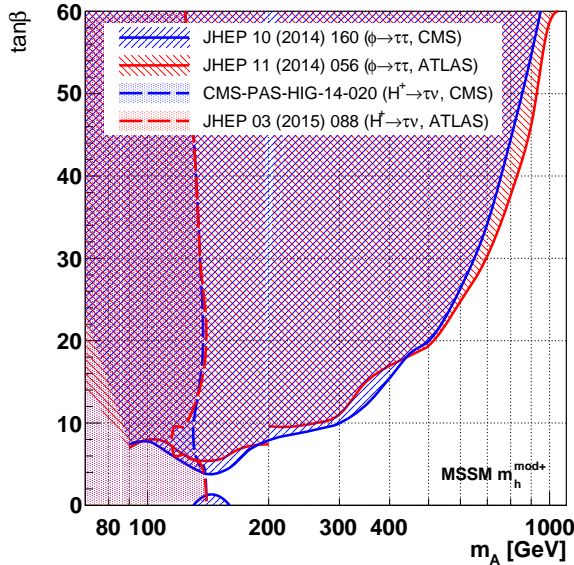


Figure 2: Regions of the  $(m_A, \tan\beta)$  plane excluded by the ATLAS and CMS collaborations in direct searches for neutral and charged Higgs bosons decaying to  $\tau$  leptons [6–9], in the benchmark MSSM scenario  $m_h^{\text{mod}+}$  described in Ref. [12].

entering the radiative corrections to satisfy the mass constraint in Eq. (8). For  $\tan\beta$  in the low single digits, the required hierarchy between  $m_{\text{SUSY}}$  and  $m_t$  is so large that a fixed-order result such as the one in Eq. (7) would be inadequate even if extended to two- or three-loop accuracy, because the un-computed higher-order corrections contain higher powers of the large logarithm of  $m_{\text{SUSY}}/m_t$ . In this case, the large logarithmic corrections to the Higgs masses should be *resummed* to all orders via an effective-field-theory (EFT) approach: the heavy SUSY particles are integrated out at the scale  $m_{\text{SUSY}}$ , where appropriate boundary conditions, free of logarithmic enhancements, are imposed on the quartic Higgs couplings; the latter are evolved down to the weak scale with the corresponding renormalization group equations (RGE); finally, the Higgs masses are computed from the quartic Higgs couplings, including the radiative corrections due to the contributions of the remaining light particles at the weak scale.

An EFT calculation of the MSSM Higgs masses in scenarios where all the SUSY particles (except possibly charginos and neutralinos) are far above the TeV scale, while all Higgs bosons are below it, is being completed [15], extending the earlier work in Ref. [16] to the case of two light Higgs doublets. The boundary conditions on the quartic couplings are computed at two loops, and the RG evolution is performed at two or three loops (the latter only in the region where the relevant effective theory is the SM). However, no public code implementing the results of such a calculation is currently available. For the analysis of low- $\tan\beta$  scenarios by ATLAS and CMS, this limitation has been circumvented in two ways: (i) in the phenomenological “hMSSM” approach of Refs. [17–19], which will be briefly described in section 2.1, the experimental knowledge of  $m_h$  can be traded – under certain assumptions – for the calculation of the radiative corrections, and used to predict the remaining masses and couplings of the MSSM Higgs bosons; (ii) in an alternative approach [20], the accurate fixed-order calculation of the MSSM Higgs masses provided by the code `FeynHiggs` [10, 21–23] has been supplemented with a partial resummation of the large logarithmic corrections [24], and used to produce a new benchmark scenario with  $m_A \leq 500$  GeV,  $\tan\beta \leq 10$  and sufficiently heavy SUSY particles,

whose predictions for  $m_h$  are compatible with the requirement of Eq. (8). This scenario, referred to as “low-tb-high”, will be briefly described in section 2.2.

In this document, the two above-mentioned approaches to the study of MSSM scenarios with low  $\tan\beta$ , light Higgs bosons and heavy SUSY are described. Each approach is introduced with its underlying assumptions and main features, and its applicability over the MSSM parameter space is discussed, also relying on a comparison with preliminary results of the EFT calculation. The computation of production cross sections and decays of the neutral Higgs bosons in the two approaches is described (ROOT files for the results can be downloaded from the web pages of the LHC-HXSWG [25]). Finally, the predictions for the Higgs decays obtained within the two approaches are compared, and the origin of some observed discrepancies is discussed.

## 2 Benchmark scenarios for low $\tan\beta$ in the MSSM

### 2.1 The hMSSM approach

In the hMSSM approach [17–19], the Higgs sector of the MSSM is described in terms of just the parameters entering the tree-level expressions for masses and mixing, Eqs. (3) and (4), plus the experimentally known value of  $m_h$ . In this sense, the hMSSM approach can be considered “model independent”, because the predictions for the properties of the MSSM Higgs bosons do not depend – with some caveats which will be discussed below – on the details of the unobserved SUSY sector.

The mass matrix for the neutral  $CP$ -even states can be decomposed as

$$\mathcal{M}_{\Phi}^2 = \mathcal{M}_{\text{tree}}^2 + \begin{pmatrix} \Delta\mathcal{M}_{11}^2 & \Delta\mathcal{M}_{12}^2 \\ \Delta\mathcal{M}_{12}^2 & \Delta\mathcal{M}_{22}^2 \end{pmatrix}, \quad (10)$$

where the tree-level matrix  $\mathcal{M}_{\text{tree}}^2$  is given in Eq. (2), and  $\Delta\mathcal{M}_{ij}^2$  are the radiative corrections. The hMSSM approach is based on the following assumptions: (i) the observed Higgs boson is the light scalar  $h$ ; (ii) of the radiative corrections in Eq. (10), only the element  $\Delta\mathcal{M}_{22}^2$ , which contains the leading logarithmic terms arising from top and stop loops, needs to be taken into account; (iii) all SUSY particles are heavy enough to escape detection at the LHC, and their effects on the Higgs sector other than those on the mass matrix, e.g. via direct loop corrections to the Higgs-boson couplings or via modifications of the total decay widths, can be neglected.

With these assumptions  $\Delta\mathcal{M}_{22}^2$  can be traded for the known value of  $m_h$ , inverting the relation that gives the lightest eigenvalue of the mass matrix in Eq. (10):

$$\Delta\mathcal{M}_{22}^2 = \frac{m_h^2 (m_A^2 + m_Z^2 - m_h^2) - m_A^2 m_Z^2 \cos^2 2\beta}{m_Z^2 \cos^2 \beta + m_A^2 \sin^2 \beta - m_h^2}, \quad (11)$$

which leads to the following expressions for the heavy-scalar mass and for the mixing angle

$$m_H^2 = \frac{(m_A^2 + m_Z^2 - m_h^2)(m_Z^2 \cos^2 \beta + m_A^2 \sin^2 \beta) - m_A^2 m_Z^2 \cos^2 2\beta}{m_Z^2 \cos^2 \beta + m_A^2 \sin^2 \beta - m_h^2}, \quad (12)$$

$$\tan \alpha = -\frac{(m_Z^2 + m_A^2) \cos \beta \sin \beta}{m_Z^2 \cos^2 \beta + m_A^2 \sin^2 \beta - m_h^2}. \quad (13)$$

The mass of the charged scalars coincides with the tree-level value  $m_{H^\pm}^2 = m_A^2 + m_W^2$  in this approximation. The couplings of the neutral Higgs bosons to fermions and to gauge bosons are fixed to their tree-level form as in Eq. (5), but they are expressed in terms of the effective

(i.e., loop-corrected) angle  $\alpha$  obtained in Eq. (13). In contrast, the triple and quartic Higgs self-couplings receive additional contributions. In particular, the effective  $Hhh$  coupling in the hMSSM reads

$$\lambda_{Hhh} = \lambda_{Hhh, \text{tree}} + 3 \frac{\Delta\mathcal{M}_{22}^2}{m_Z^2} \frac{\sin\alpha}{\sin\beta} \cos^2\alpha, \quad (14)$$

where the tree-level coupling, see Eq. (6), is also expressed in terms of the effective  $\alpha$ , and the correction  $\Delta\mathcal{M}_{22}^2$  is given in Eq. (11). Under the assumptions that characterize the hMSSM, the information encoded in Eqs. (12)–(14) is sufficient to determine the production cross sections and the decay branching ratios of all the MSSM Higgs bosons, as function of only  $m_A$  and  $\tan\beta$  for a fixed value of the light-scalar mass (which we can take as  $m_h = 125$  GeV). The precise calculation of these observables will be described in section 2.3 below.

It should be noted that the hMSSM approach is well defined only in the region of the  $(m_A, \tan\beta)$  plane where the denominator in Eqs. (11)–(13) is greater than zero (indeed, as the denominator approaches zero  $\Delta\mathcal{M}_{22}^2$  diverges, and we get  $\alpha \rightarrow -\pi/2$  and  $m_H \rightarrow \infty$ ). In other words, for any given value of  $\tan\beta$  there is a minimum value  $m_A^{\min}$  below which it is not possible to reproduce the desired  $m_h$  with only a correction to the  $(2, 2)$  element of the Higgs mass matrix. For large  $\tan\beta$  one has  $m_A^{\min} \approx m_h$ , while for decreasing  $\tan\beta$  the minimum value of  $m_A$  increases, up to  $m_A^{\min} = (2m_h^2 - m_Z^2)^{1/2}$  for  $\tan\beta = 1$  (for  $m_h = 125$  GeV, this corresponds to  $m_A^{\min} \approx 151$  GeV). However, in Ref. [19] it is argued that the region where the hMSSM approach breaks down is already excluded, both by direct searches for  $H^\pm$  and  $A$  at the LHC and by the requirement that the couplings of  $h$  be approximately SM-like.

The validity of the assumption (ii), that  $\Delta\mathcal{M}_{11}^2$  and  $\Delta\mathcal{M}_{12}^2$  can be neglected, is also discussed in Refs. [18, 19]. Direct inspection of the dominant one-loop contributions from top/stop loops shows that the corrections to the  $(1, 1)$  and  $(1, 2)$  elements of the Higgs mass matrix are proportional to powers of the ratio  $\mu X_t/m_{\text{SUSY}}^2$ . Since the sbottom contributions to those matrix elements are not enhanced at the moderate  $\tan\beta$  values of interest here, the assumption (ii) is satisfied as soon as  $\mu X_t/m_{\text{SUSY}}^2$  is suppressed. In MSSM scenarios with  $m_{\text{SUSY}}$  up to a few TeV, the inclusion of the full one-loop contributions and of the known two-loop contributions does not alter this picture. This was shown in Refs. [18, 19] via numerical comparisons between the predictions for  $m_H$  and  $\alpha$  obtained with the codes `SuSpect` [26] and `FeynHiggs` [10, 21–24] and those obtained with the hMSSM approximations, Eqs. (12) and (13), using the values of  $m_h$  produced by the codes as input. To extend this check to the very large values of  $m_{\text{SUSY}}$  required to obtain the observed value of  $m_h$  at low  $\tan\beta$ , a comparison against the proper EFT calculation would be necessary. Preliminary studies in this direction [15] indicate that, even in such heavy-SUSY scenarios, the predictions of Eqs. (12)–(14) agree within a few percent with the exact results for  $m_H$ ,  $\alpha$  and  $\lambda_{Hhh}$ , as long as  $\mu X_t/m_{\text{SUSY}}^2 \lesssim 1$ .

Concerning the assumption (iii), i.e. the absence of direct SUSY corrections to the Higgs couplings, we recall that the couplings to bottom quarks are subject to potentially large,  $\tan\beta$ -enhanced SUSY corrections – often called  $\Delta_b$  corrections – which do not decouple in the limit of heavy superparticles. However, those corrections are not particularly relevant at the values of  $\tan\beta$  considered here, and in addition they scale like  $\mu/m_{\text{SUSY}}$ , i.e. they could be suppressed by the same choices of SUSY parameters that guarantee the validity of the assumption (ii).

## 2.2 The “low-tb-high” scenario

The second approach [20] to the study of low- $\tan\beta$  scenarios in the MSSM is essentially orthogonal to the one outlined in the previous section. Instead of treating  $m_h$  as an input, and using it to obtain a simple but approximate description of the Higgs sector which is largely independent of the underlying SUSY parameters, one looks for choices of SUSY parameters that, using a



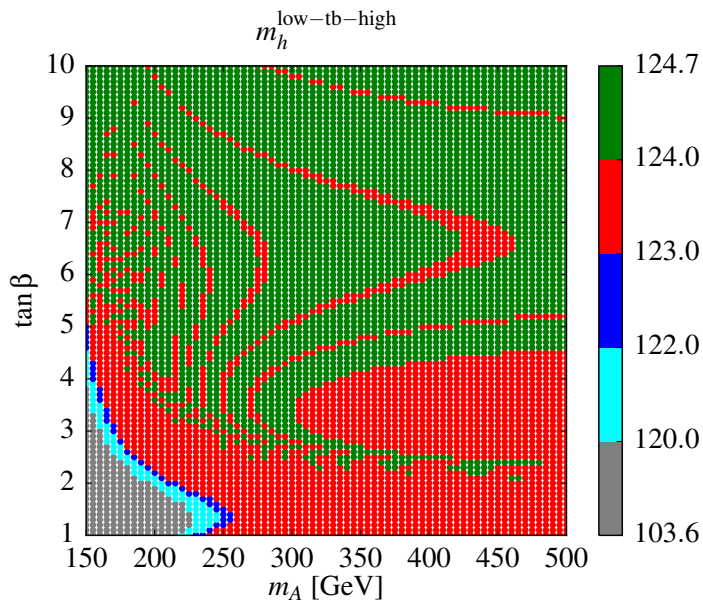


Figure 3: Mass of the light scalar  $h$  as computed by `FeynHiggs 2.10.4` in the “low-tb-high” scenario, as a function of  $m_A$  and  $\tan\beta$ .

high-precision calculation of the Higgs masses and mixing, allow to obtain the desired value of  $m_h$  in most of the  $(m_A, \tan\beta)$  plane.

As discussed in section 1, for low  $\tan\beta$  the values of  $m_{\text{SUSY}}$  required to obtain  $m_h \approx 125$  GeV are so large that a fixed-order calculation of the Higgs masses becomes inadequate, and a resummation of the large logarithmic corrections is unavoidable. Starting from version 2.10.0, the public code `FeynHiggs` [10, 21–23] does include such resummation [24], with some limitations that will be discussed below. The so-called “low-tb-high” scenario is defined for  $0.5 \leq \tan\beta \leq 10$  and  $150 \text{ GeV} \leq m_A \leq 500 \text{ GeV}$ , and the masses and mixing of all the MSSM Higgs bosons are computed with version 2.10.4 of `FeynHiggs`.

To obtain values of  $m_h$  in the desired range, the SUSY parameters – in the on-shell scheme adopted by `FeynHiggs` – are chosen as follows: (i) all soft SUSY-breaking masses for the sfermions (both squarks and sleptons) as well as the gluino mass are set equal to  $m_{\text{SUSY}}$ ; (ii)  $m_{\text{SUSY}}$  is varied between few TeV (for large values of  $m_A$  or  $\tan\beta$ ) and up to 100 TeV (for small values of  $m_A$  or  $\tan\beta$ ), keeping the following relations between  $X_t$ ,  $m_{\text{SUSY}}$  and  $\tan\beta$ :

$$\begin{aligned}
 \tan\beta \leq 2 & : & X_t/m_{\text{SUSY}} &= 2; \\
 2 < \tan\beta \leq 8.6 & : & X_t/m_{\text{SUSY}} &= 0.0375 \tan^2 \beta - 0.7 \tan \beta + 3.25; \\
 8.6 < \tan\beta & : & X_t/m_{\text{SUSY}} &= 0;
 \end{aligned}$$

(iii) for what concerns the remaining SUSY parameters, all Higgs-sfermion trilinear couplings other than  $A_t$  are set to 2 TeV,  $\mu$  is set to = 1.5 TeV and the  $SU(2)$  gaugino mass  $M_2$  is set to 2 TeV (this fixes also the  $U(1)$  gaugino mass  $M_1$  via the GUT relation  $M_1/M_2 = 5/3 \tan^2 \theta_W$ ). With these choices of SUSY parameters, the prediction of `FeynHiggs` for the light-scalar mass  $m_h$  is shown in Figure 3 as a function of  $m_A$  and  $\tan\beta$ . As can be seen, the requirement of Eq. (8) can be met over most of the parameter space, with the exception of the lower-left corner corresponding to very low values of both  $m_A$  and  $\tan\beta$ . However, it has not been tested whether the predictions for the production cross section and the branching ratios of the light scalar are in full agreement with the latest results of the ATLAS and CMS collaborations [4, 5], which indicate

a SM-like Higgs boson with uncertainties in the (10–20)% range. For the heavy Higgs bosons, the chosen values of  $\mu$  and  $M_2$  ensure that all decays to charginos and neutralinos (henceforth, electroweakinos or EW-inos) are kinematically closed, thus maximizing the branching ratios for the decays in Eq. (9).

A limitation of the “low-tb-high” scenario should be taken into account. The resummation procedure currently implemented in `FeynHiggs` – which accounts only for the leading and next-to-leading logarithmic corrections to the Higgs masses controlled by the strong gauge coupling and by the top Yukawa coupling – relies on the assumption that all SUSY masses as well as the heavy-Higgs masses are of the order of  $m_{\text{SUSY}}$ . However, in the “low-tb-high” scenario the parameters  $\mu$  and  $M_{1,2}$  are fixed to  $\mathcal{O}(\text{TeV})$ , and  $m_A$  is below 500 GeV. To assess the adequacy of `FeynHiggs` in an MSSM scenario with heavy sfermions and gluinos but relatively light EW-inos and additional Higgs bosons, a comparison with a proper EFT calculation – where the effective theory below  $m_{\text{SUSY}}$  is a two-Higgs-doublet model (THDM) augmented with EW-inos – would be necessary.

Preliminary studies in this direction [15] indicate that, with the choices of SUSY parameters of the “low-tb-high” scenario, the EFT predictions for  $m_h$  can be considerably lower than those of the current `FeynHiggs` implementation. In particular, for  $\tan\beta > 5.5$  the EFT calculation yields values of  $m_h$  that are about 2 GeV lower than those obtained by `FeynHiggs`. For lower values of  $\tan\beta$ , the disagreement is more severe: the difference is greater than 5 GeV (10 GeV) for  $\tan\beta < 3.5$  ( $\tan\beta < 2$ ). When one looks at the minimal value of  $m_{\text{SUSY}}$  required to obtain  $m_h$  in the desired range, the logarithmic dependence of  $m_h$  on  $m_{\text{SUSY}}$  amplifies the discrepancy. For  $\tan\beta = 2$ , the EFT calculation requires  $m_{\text{SUSY}} > 10^8$  TeV ( $m_{\text{SUSY}} > 200$  TeV) to obtain  $m_h > 122$  GeV with  $m_A = 200$  GeV ( $m_A = 500$  GeV). This should be compared with the maximal value  $m_{\text{SUSY}} = 100$  TeV adopted in the “low-tb-high” scenario for the lowest values of  $m_A$  and  $\tan\beta$ . Discrepancies up to (10–12)% between `FeynHiggs` and the EFT calculation can also be found in the predictions for  $m_H$  and  $\alpha$  at very small values of  $m_A$  and  $\tan\beta$ . Further investigation will be required to ascertain how these discrepancies are related to the presence of a light THDM, to the presence of light EW-inos, and to other aspects of the calculation such as the determination of the top Yukawa coupling.

On the other hand, the fact that  $\mu \ll m_{\text{SUSY}}$  over the whole parameter space ensures that the dominant top/stop corrections to the elements other than (2, 2) of the  $CP$ -even Higgs mass matrix are suppressed. Therefore, a meaningful comparison with the results obtained in the hMSSM approach can be performed, as will be discussed in section 2.4.

### 2.3 Cross sections and branching ratios

To facilitate the analysis of low- $\tan\beta$  scenarios by the ATLAS and CMS collaborations, `ROOT` files have been produced for both the hMSSM approach and the “low-tb-high” scenario, providing the production cross sections and the decay branching ratios of all the neutral MSSM Higgs bosons, for a grid of values of  $m_A$  and  $\tan\beta$ . In particular, results were produced in the ranges  $150 \text{ GeV} \leq m_A \leq 500 \text{ GeV}$  and  $0.5 \leq \tan\beta \leq 10$  for the “low-tb-high” scenario, and  $130 \text{ GeV} \leq m_A \leq 1 \text{ TeV}$  and  $1 < \tan\beta \leq 60$  for the hMSSM. In the latter, however, some points at low  $m_A$  and low  $\tan\beta$  are discarded by requirement that the denominator in Eqs. (11)–(13) be positive, and the points with  $\tan\beta > 10$  or  $m_A > 500$  GeV are not relevant to this discussion. In the hMSSM files the mass of the light neutral scalar has been fixed to  $m_h = 125$  GeV, then  $m_H$  and  $\alpha$  have been computed as function of  $m_A$  and  $\tan\beta$  using Eqs. (12) and (13). In contrast, in the “low-tb-high” files both neutral-scalar masses, as well as  $\alpha$ , have been computed with `FeynHiggs 2.10.4`, starting from the SUSY parameter choices that define the scenario and from the SM input parameters listed in appendix A. As shown in Figure 3, this implies that in the

“low-tb-high” files  $m_h$  is not fixed to a constant value over the  $(m_A, \tan\beta)$  plane.

The cross sections for the production of the neutral Higgs bosons  $\phi \equiv (h, H, A)$  via gluon fusion ( $gg \rightarrow \phi$ ) and bottom annihilation ( $b\bar{b} \rightarrow \phi$ ), for center-of-mass energies of both 8 TeV and 13 TeV, have been computed with the code `SusHi` 1.5.0 [27]. For gluon fusion, the code implements the full top- and bottom-loop contributions at NLO in QCD from Refs. [28, 29], NNLO-QCD top contributions in the heavy-top limit from Refs. [30, 31] (see also Refs. [32–34]), and electroweak contributions by light quarks from Refs. [35, 36]. In the case of the hMSSM, no contributions from squark loops are included, consistent with the assumption (iii) of that approach. For what concerns the “low-tb-high” scenario, the squark-loop contributions to the gluon-fusion amplitude could in principle be computed by `SusHi`, but they are negligible even for the lowest considered values of  $m_{\text{SUSY}}$ . Those contributions have therefore been omitted, in order to improve the numerical stability of the calculation. On the other hand, the non-decoupling  $\Delta_b$  corrections to the Higgs-bottom couplings are included in the “low-tb-high” scenario, but their effect for  $\tan\beta < 10$  is not significant.

For bottom annihilation, `SusHi` implements the NNLO-QCD results in the five-flavor scheme from Ref. [37]. For each neutral Higgs boson  $\phi$ , the amplitude for the production of a SM Higgs boson of mass  $m_\phi$  is reweighted with the effective coupling  $g_{dd}$  given in Eq. (5). Also in this case, the  $\Delta_b$  corrections are included only in the “low-tb-high” scenario. In addition, the `ROOT` files contain reweighted four-flavor-scheme cross sections for bottom-quark associated production ( $gg \rightarrow b\bar{b}\phi$ ) [38, 39], as well as the “Santander matched” cross sections which combine the five-flavor and four-flavor descriptions of the process [40].

In the calculation of the cross sections, the SM input parameters for `SusHi` have been set to the values listed in appendix A. The renormalization scale  $\mu_R$  and the factorization scale  $\mu_F$  have been fixed as  $\mu_R = \mu_F = m_\phi/2$  in the case of gluon fusion and as  $\mu_R = 4\mu_F = m_\phi$  in the case of bottom annihilation. Scale uncertainties have been obtained from the envelope of seven independent variations of  $\mu_R$  and  $\mu_F$  by factors of 2 with the constraint  $1/2 \leq \mu_R/\mu_F \leq 2$  in the case of gluon fusion and  $2 \leq \mu_R/\mu_F \leq 8$  in the case of bottom annihilation. For the parton distribution functions the `MSTW2008` [41] set has been used, and the residual uncertainties on the parton distribution functions and on the strong coupling constant,  $\alpha_s$ , have been obtained from the corresponding relative uncertainties for a SM Higgs boson of mass  $m_\phi$ , evaluated as proposed in Ref. [42].

Concerning the calculation of the branching ratios, there are important differences between the hMSSM files and the “low-tb-high” files. In the hMSSM files, the branching ratios for the decays of the neutral Higgs bosons are computed with the code `HDECAY` [43, 44], which – starting from version 6.40 – can take  $m_h$  as input and obtain  $m_H$  and  $\alpha$  from the hMSSM prescriptions in Eqs. (12) and (13). The values of the SM input parameters used by the code are listed in appendix A. For the decays relevant to this discussion, the hMSSM mode of `HDECAY` implements: N<sup>4</sup>LO-QCD corrections to the decays to quark pairs [45–58]; LO results for the decays to lepton pairs and for the decays involving massive gauge bosons, both on-shell and off-shell; a LO calculation of the decays to Higgs-boson pairs, both on-shell and off-shell, using effective hMSSM couplings such as the  $Hhh$  coupling in Eq. (14). In contrast, in the `ROOT` files for the “low-tb-high” scenario the branching ratios have been computed as recommended by the LHC-HXSWG [59], by combining the results of `HDECAY` for the decays to quark pairs with the results of `FeynHiggs` for the remaining decays. In particular, for the decays to massive gauge bosons `FeynHiggs` approximates the MSSM results by reweighting the SM results from the code `PROPHECY4f` [60, 61] with the effective couplings  $g_{VV}$  given in Eq. (5). For the decays to Higgs bosons, `FeynHiggs` implements a full one-loop calculation within the (complex) MSSM [62], improved – starting from version 2.10.4 – with the resummation of potentially large logarithmic corrections to the decay  $H \rightarrow hh$ .

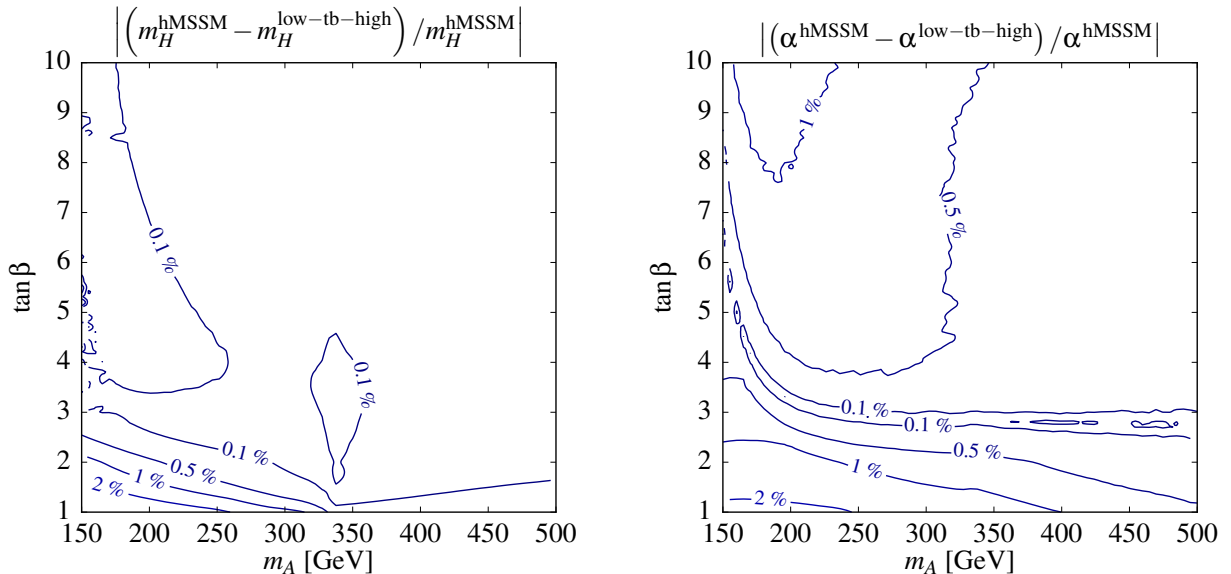


Figure 4: Relative differences in  $m_H$  (left) and  $\alpha$  (right) between the predictions of `FeynHiggs` for the “low-tb-high” scenario and the corresponding predictions obtained in the hMSSM approach via Eqs. (12) and (13), starting from the values of  $m_h$  computed by `FeynHiggs`.

## 2.4 Comparing the predictions for the Higgs-boson properties

As mentioned in section 2.2, the choices of SUSY parameters in the “low-tb-high” scenario satisfy all of the assumptions that underlie the hMSSM, thus inviting a comparison between the predictions for the Higgs-boson properties obtained within the two approaches. However, a direct comparison between the two sets of `ROOT` files is hindered by the fact that the light-scalar mass is fixed as  $m_h = 125$  GeV in the hMSSM files, whereas it varies with  $m_A$  and  $\tan\beta$  in the “low-tb-high” files. To circumvent this problem, we compared the predictions of the “low-tb-high” scenario for  $m_H$ ,  $\alpha$  and the branching ratios with the corresponding results obtained in the hMSSM approach taking as input the values of  $m_h$  from the “low-tb-high” scenario and computing all branching ratios with `HDECAY`.

In the left and right panels of Figure 4 we show the relative differences between the predictions of the “low-tb-high” scenario and those of the hMSSM for  $m_H$  and  $\alpha$ , respectively, on the  $(m_A, \tan\beta)$  plane with  $150 \text{ GeV} \leq m_A \leq 500 \text{ GeV}$  and  $1 \leq \tan\beta \leq 10$ . The figure shows that, for the SUSY parameters that characterize the “low-tb-high” scenario, the results of `FeynHiggs` for  $m_H$  and  $\alpha$  and the approximate results obtained via Eqs. (12) and (13) differ by less than 1% over most of the parameter space. Larger discrepancies, up to a few percent, occur only in the lower-left corner at very low  $m_A$  and  $\tan\beta$ . In view of this good accord, we can expect any significant discrepancy in the predictions for cross sections and branching ratios to be due to differences in the calculation of the physical observables themselves, rather than to the approximation in Eqs. (12) and (13). While the production cross sections are computed with `SusHi` in both cases, discrepancies can arise in the widths for the decays in Eq. (9), which in the “low-tb-high” and hMSSM files are computed with `FeynHiggs+PROPHECY4f` and with `HDECAY`, respectively.

The left and right panels in Figure 5 show the branching ratio for the decay  $H \rightarrow hh$  in the “low-tb-high” scenario and in the hMSSM+`HDECAY` combination, respectively. Again, in the hMSSM plot the mass  $m_h$  used to compute  $m_H$  and  $\alpha$  via Eqs. (12) and (13) in a given point of the  $(m_A, \tan\beta)$  plane has been adjusted to the value computed by `FeynHiggs` in the

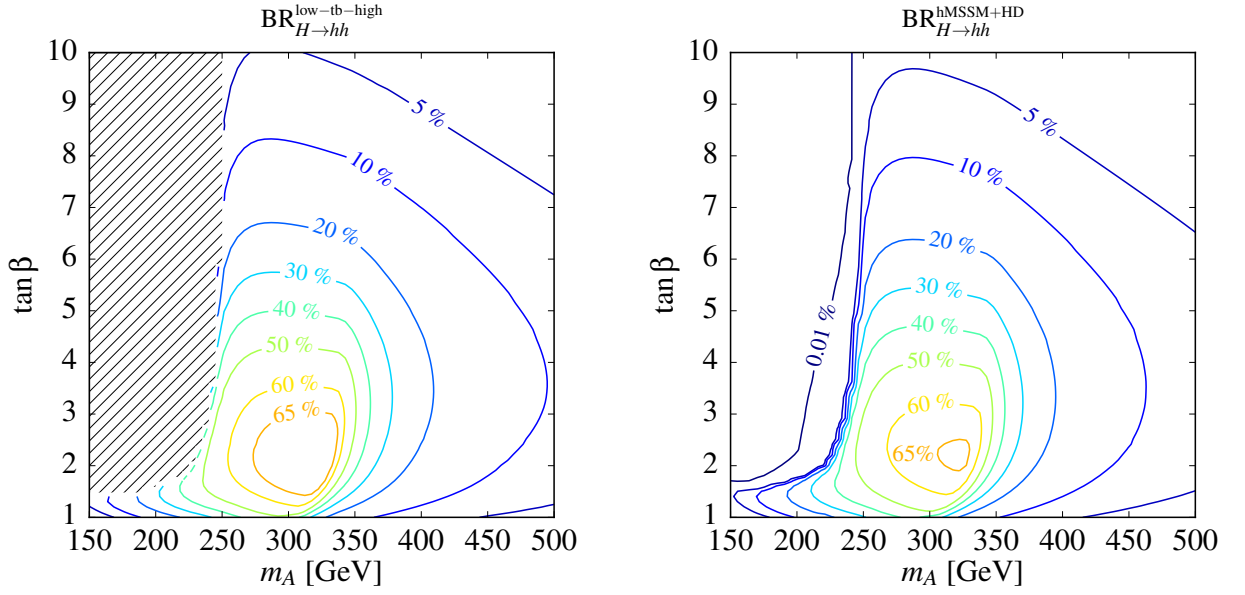


Figure 5: Left: Branching ratio for the decay  $H \rightarrow hh$  as computed in the “low-tb-high” scenario following the LHC-HXSWG recommendations for the decay widths (in particular,  $\Gamma(H \rightarrow hh)$  is computed with `FeynHiggs`). Right: The same branching ratio obtained with the hMSSM+HDECAY combination – namely, starting from the values of  $m_h$  computed by `FeynHiggs` in the “low-tb-high” scenario, then computing the branching ratio with HDECAY, which obtains  $m_H$ ,  $\alpha$  and  $\lambda_{Hhh}$  from the hMSSM prescriptions in Eqs. (12)–(14).

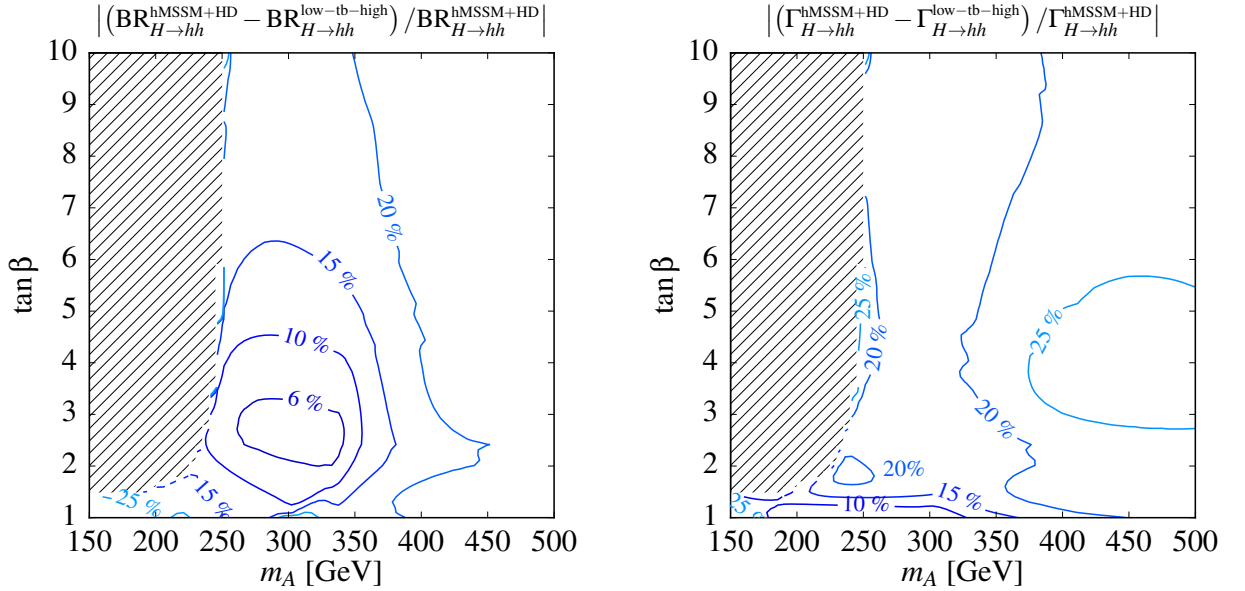


Figure 6: Relative differences in  $\text{BR}(H \rightarrow hh)$  (left) and  $\Gamma(H \rightarrow hh)$  (right) between the predictions of the “low-tb-high” scenario (where  $\Gamma(H \rightarrow hh)$  is computed with `FeynHiggs`) and the corresponding predictions obtained with the hMSSM+HDECAY combination. For the latter we start from the values of  $m_h$  computed by `FeynHiggs` in the “low-tb-high” scenario, then we compute width and branching ratio with HDECAY, which obtains  $m_H$ ,  $\alpha$  and  $\lambda_{Hhh}$  from the hMSSM prescriptions in Eqs. (12)–(14).

corresponding point of the “low-tb-high” scenario. In the hatched region on the left plot the decay is below threshold, and the corresponding width is set to zero by `FeynHiggs` (in contrast, in the right plot `HDECAY` computes also the small width to off-shell scalars). The plots show that, in this scenario,  $\text{BR}(H \rightarrow hh)$  can be larger than 50% for  $\tan \beta \lesssim 4$  and for values of  $m_A$  such that  $m_H$  sits between the kinematic threshold for the decay to a light-scalar pair and the one for the decay to a top-quark pair. A visual comparison of the left and right plots also shows that the qualitative dependence of  $\text{BR}(H \rightarrow hh)$  on  $m_A$  and  $\tan \beta$  is the same in both approaches, but the branching ratio takes on somewhat larger values in the “low-tb-high” plot than it does in the hMSSM plot.

To quantify the previous statement, the left plot in Figure 6 shows the relative difference between the values of  $\text{BR}(H \rightarrow hh)$  computed in the “low-tb-high” scenario and those computed in the hMSSM with `HDECAY`. The plot shows that the discrepancy in the branching ratio is less than 10% in the region where the decay  $H \rightarrow hh$  is dominant, and exceeds 20% for larger values of  $m_A$  and, hence,  $m_H$ . However, in the region where a decay channel is dominant a comparison between branching ratios can mask the true extent of a discrepancy. The right plot of Figure 6 shows instead the relative difference between the corresponding values of the decay width  $\Gamma(H \rightarrow hh)$ . It appears that, at the level of the decay width, the discrepancy between the results obtained in the two approaches is above 15% in most of the relevant parameter space, and exceeds 25% for large  $m_A$  and intermediate  $\tan \beta$ . The size of the discrepancy can be understood in view of the different accuracy of the  $\Gamma(H \rightarrow hh)$  calculation in the two approaches. Indeed, while in the hMSSM the effect of the top/stop contributions is included via the effective coupling in Eq. (14), `FeynHiggs` implements a full calculation of the one-loop corrections to the decay width, supplemented with the resummation of large logarithmic terms. Thus, the `FeynHiggs` result accounts for potentially large threshold effects in diagrams with loops of SM particles, which are not captured by using an effective coupling alone.

In Figures 7–12 we show plots analogous to those in Figures 5 and 6, for the decays  $H \rightarrow WW$ ,  $H \rightarrow ZZ$  and  $A \rightarrow Zh$ . For what concerns the decays of  $H$  to massive gauge-boson pairs, the relative differences between the two calculations of the widths are – over most of the  $(m_A, \tan \beta)$  plane – smaller than 15% for  $WW$  and smaller than 10% for  $ZZ$ . Again, such discrepancies can be explained by the fact that, in the “low-tb-high” files, the  $H \rightarrow VV$  decay widths are obtained by reweighting the state-of-the-art SM results of `PROPHECY4f`, whereas in the hMSSM files those widths are computed at LO with `HDECAY`. For the decay  $A \rightarrow Zh$ , Figure 12 shows that – in the region with  $m_A > m_Z + m_h$  where the decay is kinematically open – the relative differences between the two calculations of the widths are smaller than 10% unless  $\tan \beta$  is very close to 1. For lower values of  $m_A$ , where the pseudoscalar must decay to off-shell bosons, large discrepancies appear, due to differences in both the implementation of the calculations and the input value of  $\alpha$ . However, the decay width is extremely suppressed in that region, and the process is not relevant to the low- $\tan \beta$  analysis.

Finally, we performed analogous comparisons for all the remaining decay channels of  $H$  and  $A$ , but we discuss here only the decays to pairs of third-family SM fermions, which can reach sizeable branching ratios in the considered scenario. The widths for the decays to top and bottom pairs are computed with `HDECAY` in both approaches, therefore any discrepancy must be due to different input values for  $m_H$  and  $\alpha$ . For the decays to top quarks, we find discrepancies of  $\mathcal{O}(1\%)$  in the region where the relevant Higgs mass is above the threshold for the production of a real-top pair and the decay is unsuppressed. For the decays to bottom quarks, the discrepancies for  $\tan \beta \gtrsim 3$ , where the branching ratio becomes significant, are also of  $\mathcal{O}(1\%)$ . In contrast, the decays to tau leptons are computed at LO with `HDECAY` in the hMSSM files, and at one loop with `FeynHiggs` in the “low-tb-high” files. In this case, the discrepancies for  $\tan \beta \gtrsim 3$  are smaller than 5% for  $\Gamma(H \rightarrow \tau\tau)$ , and smaller than 8% for  $\Gamma(A \rightarrow \tau\tau)$ .

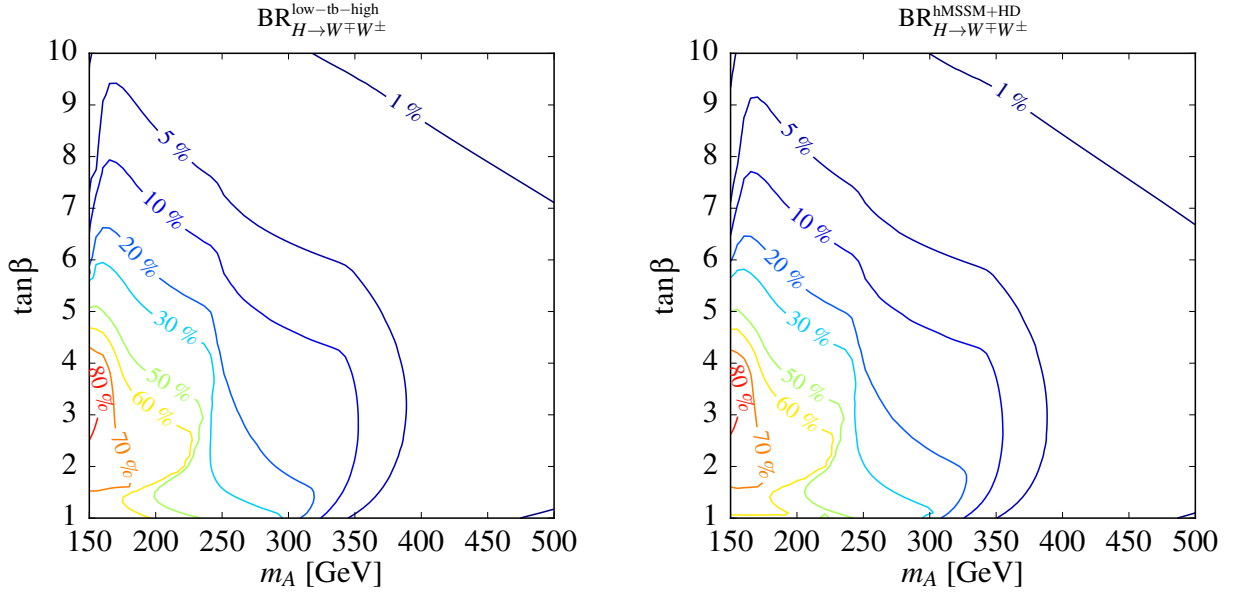


Figure 7: Left: Branching ratio for the decay  $H \rightarrow WW$  as computed in the “low-tb-high” scenario following the LHC-HXSWG recommendations for the decay widths (in particular,  $\Gamma(H \rightarrow WW)$  is computed with `FeynHiggs+PROPHECY4f`). Right: The same branching ratio obtained with the hMSSM+HDECAY combination – namely, starting from the values of  $m_h$  computed by `FeynHiggs` in the “low-tb-high” scenario, then computing the branching ratio with HDECAY, which obtains  $m_H$ ,  $\alpha$  and  $\lambda_{Hhh}$  from the hMSSM prescriptions in Eqs. (12)–(14).

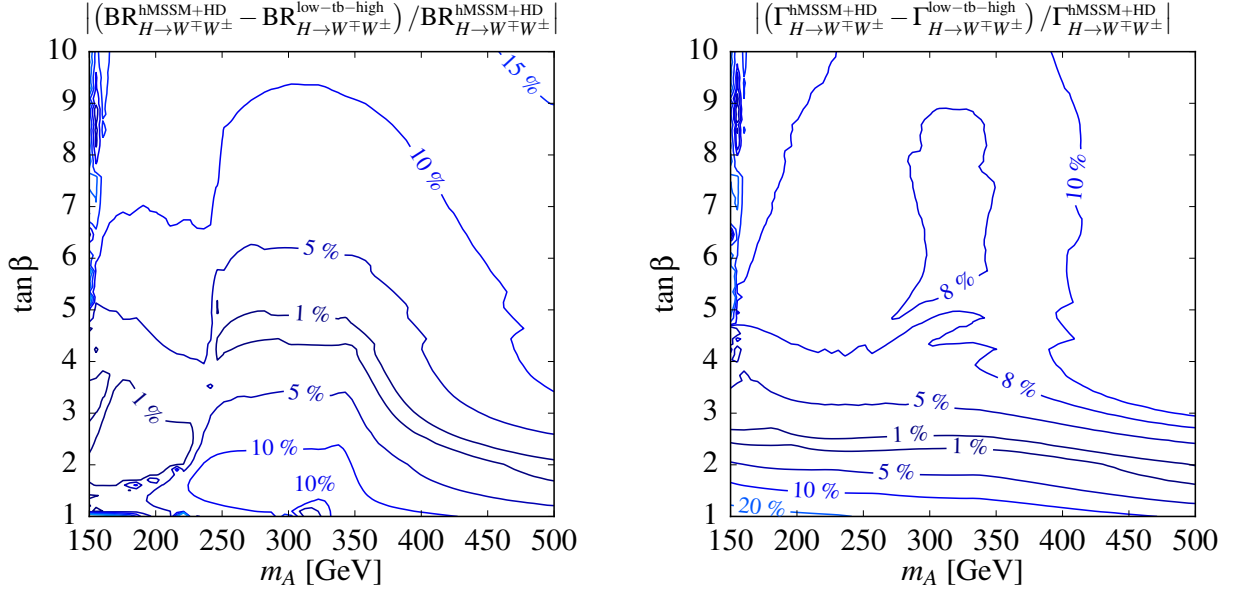


Figure 8: Relative differences in  $\text{BR}(H \rightarrow WW)$  (left) and  $\Gamma(H \rightarrow WW)$  (right) between the predictions of the “low-tb-high” scenario (where  $\Gamma(H \rightarrow WW)$  is computed with `FeynHiggs+PROPHECY4f`) and the corresponding predictions obtained with the hMSSM+HDECAY combination. For the latter we start from the values of  $m_h$  computed by `FeynHiggs` in the “low-tb-high” scenario, then we compute width and branching ratio with HDECAY, which obtains  $m_H$ ,  $\alpha$  and  $\lambda_{Hhh}$  from the hMSSM prescriptions in Eqs. (12)–(14).

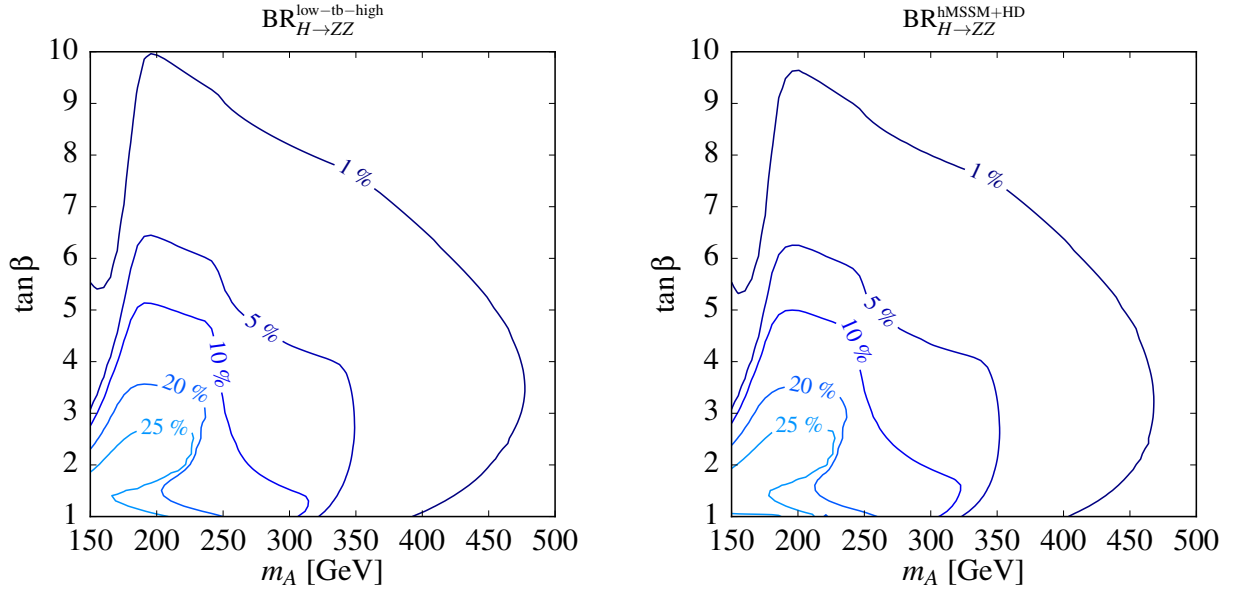


Figure 9: Left: Branching ratio for the decay  $H \rightarrow ZZ$  as computed in the “low-tb-high” scenario following the LHC-HXSWG recommendations for the decay widths (in particular,  $\Gamma(H \rightarrow ZZ)$  is computed with `FeynHiggs+PROPHECY4f`). Right: The same branching ratio obtained with the hMSSM+HDECAY combination – namely, starting from the values of  $m_h$  computed by `FeynHiggs` in the “low-tb-high” scenario, then computing the branching ratio with HDECAY, which obtains  $m_H$ ,  $\alpha$  and  $\lambda_{Hhh}$  from the hMSSM prescriptions in Eqs. (12)–(14).

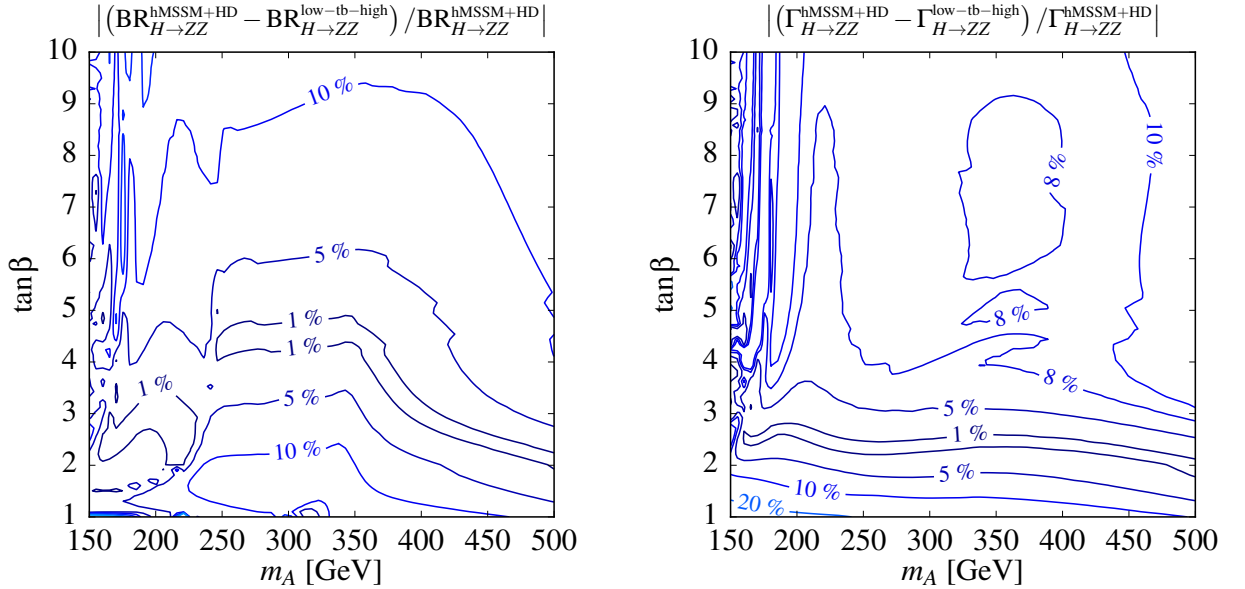


Figure 10: Relative differences in  $\text{BR}(H \rightarrow ZZ)$  (left) and  $\Gamma(H \rightarrow ZZ)$  (right) between the predictions of the “low-tb-high” scenario (where  $\Gamma(H \rightarrow ZZ)$  is computed with `FeynHiggs+PROPHECY4f`) and the corresponding predictions obtained with the hMSSM+HDECAY combination. For the latter we start from the values of  $m_h$  computed by `FeynHiggs` in the “low-tb-high” scenario, then we compute width and branching ratio with HDECAY, which obtains  $m_H$ ,  $\alpha$  and  $\lambda_{Hhh}$  from the hMSSM prescriptions in Eqs. (12)–(14).



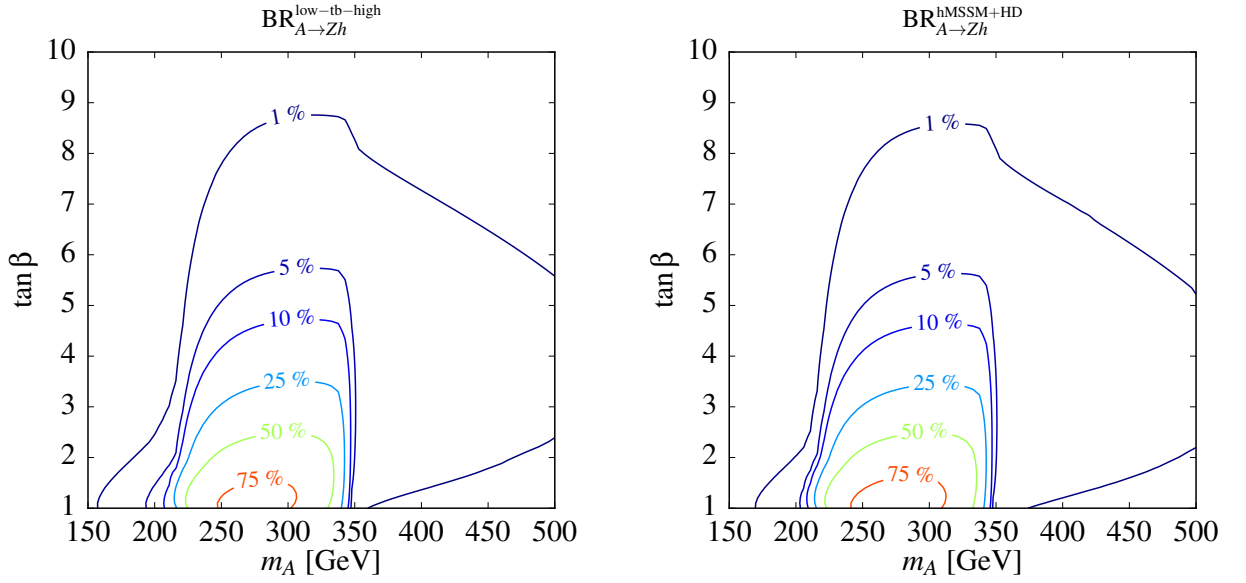


Figure 11: Left: Branching ratio for the decay  $A \rightarrow Zh$  in the “low-tb-high” scenario;  $\Gamma(A \rightarrow Zh)$  is computed with `FeynHiggs`, and the other widths are evaluated following the LHC-HXSWG recommendations. Right: The same branching ratio obtained with the hMSSM+HDECAY combination – namely, starting from the values of  $m_h$  computed by `FeynHiggs` in the “low-tb-high” scenario, then computing the branching ratio with HDECAY, which obtains  $m_H$ ,  $\alpha$  and  $\lambda_{Hhh}$  from the hMSSM prescriptions in Eqs. (12)–(14).

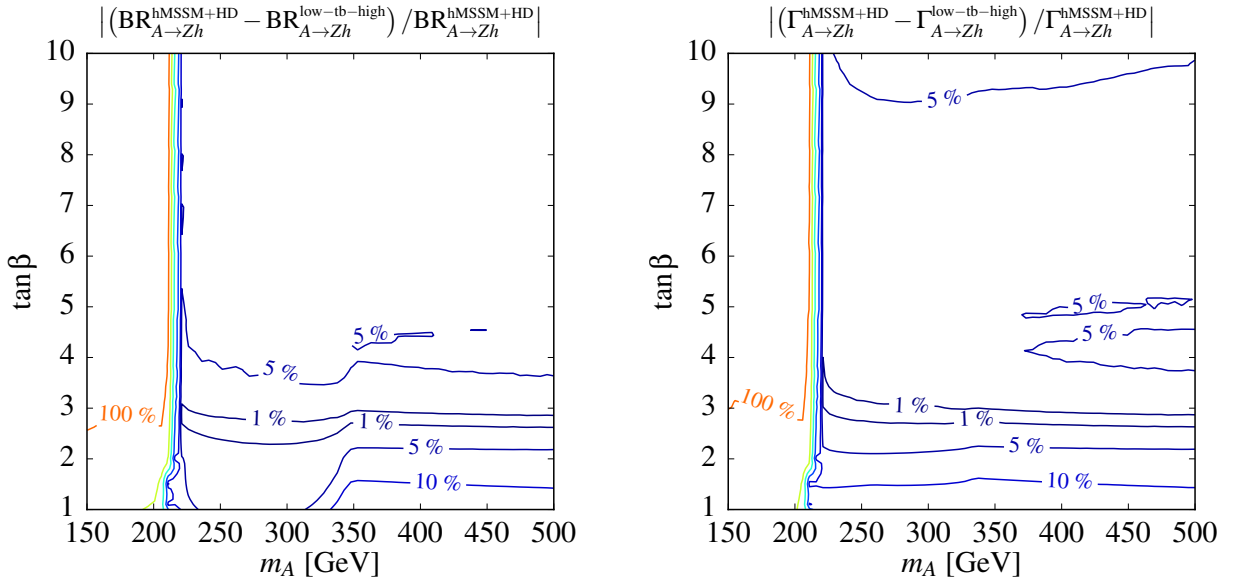


Figure 12: Relative differences in  $\text{BR}(A \rightarrow Zh)$  (left) and  $\Gamma(A \rightarrow Zh)$  (right) between the predictions of the “low-tb-high” scenario (where  $\Gamma(A \rightarrow Zh)$  is computed with `FeynHiggs`) and the corresponding predictions obtained with the hMSSM+HDECAY combination. For the latter we start from the values of  $m_h$  computed by `FeynHiggs` in the “low-tb-high” scenario, then we compute width and branching ratio with HDECAY, which obtains  $m_H$ ,  $\alpha$  and  $\lambda_{Hhh}$  from the hMSSM prescriptions in Eqs. (12)–(14).

In summary, this comparison shows that – in an MSSM scenario where its underlying assumptions are satisfied – the hMSSM approach provides a good approximation to the results of a direct calculation of the Higgs-boson properties. The observed discrepancies of order (10–20)% in the decays of Eq. (9) originate from the different accuracy in the calculations of the decay widths, and could be reduced by including in `HDECAY` the effect of EW corrections from loops of SM particles. However, we stress again that a direct comparison between the `ROOT` files for the hMSSM and those for the “low-tb-high” scenario would yield larger discrepancies than those shown in Figures 5–12, due to the different values of  $m_h$  used in the two sets of files.

### 3 Conclusions

The region of the MSSM parameter space with low  $\tan\beta$  and low  $m_A$  is characterized by a rich phenomenology in the extended Higgs sector, and is not yet excluded by the searches for exotic Higgs bosons decaying to tau pairs at the LHC. However, very heavy stops are required in this region to lift the MSSM prediction for the mass of the SM-like scalar to the observed value  $m_h \approx 125$  GeV. In the presence of widely-split mass scales, an accurate determination of the properties of the Higgs sector cannot rely on a fixed-order calculation only, but requires the resummation of large logarithmic corrections via appropriate EFT techniques.

In this document, two approaches to the study of MSSM scenarios with low  $\tan\beta$ , light Higgs bosons and heavy superparticles have been described: (i) in the hMSSM approach [17–19], the experimental knowledge of  $m_h$  is traded – under certain assumptions – for the calculation of the radiative corrections, and used to predict the remaining masses and couplings of the MSSM Higgs bosons; (ii) in an alternative approach [20], the accurate fixed-order calculation of the Higgs masses and mixing provided by `FeynHiggs` [10, 21–23], supplemented with a partial resummation of the large logarithmic corrections [24], has been used to produce a new benchmark scenario – named “low-tb-high” – whose predictions for  $m_h$  are within 3 GeV from the observed value over most of the  $(m_A, \tan\beta)$  plane.

The applicability of each approach over the MSSM parameter space has been discussed, also relying on a comparison with preliminary results of a new EFT calculation [15]. It has been found that the predictions of the hMSSM approach agree within a few percent with those of the EFT calculation, as long as an additional assumption is imposed on the unobservable parameters of the stop sector. For the “low-tb-high” scenario, it has been found that, at very low  $m_A$  and  $\tan\beta$ , the EFT predictions for the mass of the SM-like scalar are considerably lower than those of the current `FeynHiggs` implementation. This also entails discrepancies up to (10–12)% in the predictions for  $m_H$  and  $\alpha$ , relevant to the phenomenology of the heavier Higgs bosons.

For each approach, `ROOT` files containing the production cross sections and the branching ratios of the neutral Higgs bosons over the  $(m_A, \tan\beta)$  plane have been produced, and can be downloaded from the web pages of the LHC-HXSWG [25]. The mass of the SM-like scalar has been fixed to 125 GeV in the hMSSM files, whereas in the “low-tb-high” files it is computed by `FeynHiggs` in each point of the  $(m_A, \tan\beta)$  plane. The cross sections have been computed with `SusHi` [27] in both cases, while the calculations of the branching ratios rely on different sets of codes: `HDECAY` [43, 44] alone for the hMSSM, and a combination of `FeynHiggs`, `HDECAY` and `PROPHECY4f` [60, 61] for the “low-tb-high” scenario.

Finally, the predictions for the Higgs-boson properties obtained within the two approaches have been compared. After discounting for the differences in  $m_h$ , the two approaches agree at the sub-percent level in their predictions for  $m_H$  and  $\alpha$  over most of the  $(m_A, \tan\beta)$  plane. Discrepancies of order (10–20)% have been observed in the decays of the heavy Higgs bosons to gauge bosons and to SM-like scalars. Their origin is traced to the different accuracy of the codes used to compute the decay widths in the two cases.

## A SM input parameters for FeynHiggs, SusHi and HDECAY

SM input parameters for FeynHiggs 2.10.4		
Parameter	Value	
$\alpha_s(m_Z)$	0.119	
$m_c(m_c)^{\overline{\text{MS}}}$	1.28	GeV
$m_b(m_b)^{\overline{\text{MS}}}$	4.16	GeV
$m_t^{\text{pole}}$	172.5	GeV
$G_F$	$1.16637 \times 10^{-5}$	$\text{GeV}^{-2}$
$m_Z$	91.1876	GeV
$m_W$	80.398	GeV

Table 1: SM parameters used for the calculation of the MSSM Higgs boson masses, mixing angle and decay widths with the code `FeynHiggs 2.10.4`.

SM input parameters for SusHi 1.5.0		
Parameter	Value	Comment
PDF(NLO)		MSTW2008nlo68c1
PDF(NNLO)		MSTW2008nnlo68c1
$\alpha_s(m_Z)$	0.119	
$m_c(m_c)^{\overline{\text{MS}}}$	1.28	GeV
$m_b(m_b)^{\overline{\text{MS}}}$	4.16	GeV
$m_b^{\text{pole}}$	4.75	GeV
$m_t^{\text{pole}}$	172.5	GeV
$G_F$	$1.16637 \times 10^{-5}$	$\text{GeV}^{-2}$
$m_Z$	91.1876	GeV
$\alpha_{EW}^{-1}(m_Z)$	127.67	Fictitious value to obtain $m_W = 80.398$ GeV

Table 2: SM parameters used for the calculation of the Higgs production cross sections with the code `SusHi 1.5.0`. The listed value of  $\alpha_s(m_Z)$  is used for RG evolution and passed to `FeynHiggs` for the calculation of the Higgs-boson masses and mixing, whereas the cross-section calculations use the values of  $\alpha_s$  associated to the PDFs.

SM input parameters for HDECAY 6.42			
Parameter	Value		Comment
$\alpha_s(m_Z)$	0.119		
$m_c(m_c)^{\overline{\text{MS}}}$	1.28	GeV	
$m_b(m_b)^{\overline{\text{MS}}}$	4.16	GeV	
$m_c^{\text{pole}}$	1.42	GeV	1-loop value
$m_b^{\text{pole}}$	4.49	GeV	1-loop value
$m_t^{\text{pole}}$	172.5	GeV	
$G_F$	$1.16637 \times 10^{-5}$	$\text{GeV}^{-2}$	
$m_Z$	91.15349	GeV	Complex mass scheme
$m_W$	80.36951	GeV	Complex mass scheme
$\Gamma_Z$	2.49581	GeV	Derived NLO quantity
$\Gamma_W$	2.08856	GeV	Derived NLO quantity

Table 3: SM parameters used for the calculation of the Higgs decay widths with the code HDECAY 6.42.

## References

- [1] ATLAS , “Observation of a new particle in the search for the Standard Model Higgs boson with the ATLAS detector at the LHC”, *Phys.Lett.* **B716** (2012) 1–29, doi:10.1016/j.physletb.2012.08.020, arXiv:1207.7214.
- [2] CMS , “Observation of a new boson at a mass of 125 GeV with the CMS experiment at the LHC”, *Phys.Lett.* **B716** (2012) 30–61, doi:10.1016/j.physletb.2012.08.021, arXiv:1207.7235.
- [3] ATLAS, CMS , “Combined Measurement of the Higgs Boson Mass in  $pp$  Collisions at  $\sqrt{s} = 7$  and 8 TeV with the ATLAS and CMS Experiments”, *Phys.Rev.Lett.* **114** (2015) 191803, doi:10.1103/PhysRevLett.114.191803, arXiv:1503.07589.
- [4] CMS , “Precise determination of the mass of the Higgs boson and tests of compatibility of its couplings with the standard model predictions using proton collisions at 7 and 8 TeV”, *Eur.Phys.J.* **C75** (2015), no. 5, 212, doi:10.1140/epjc/s10052-015-3351-7, arXiv:1412.8662.

- [5] ATLAS Collaboration , “Measurements of the Higgs boson production and decay rates and couplings using pp collision data at  $\sqrt{s} = 7$  and 8 TeV in the ATLAS experiment”, Technical Report ATLAS-CONF-2015-007, CERN, 2015. Geneva, (Mar, 2015).
- [6] CMS , “Search for neutral MSSM Higgs bosons decaying to a pair of tau leptons in pp collisions”, *JHEP* **1410** (2014) 160, doi:10.1007/JHEP10(2014)160, arXiv:1408.3316.
- [7] ATLAS , “Search for neutral Higgs bosons of the minimal supersymmetric standard model in pp collisions at  $\sqrt{s} = 8$  TeV with the ATLAS detector”, *JHEP* **1411** (2014) 056, doi:10.1007/JHEP11(2014)056, arXiv:1409.6064.
- [8] CMS Collaboration , “Search for charged Higgs bosons with the  $H^+$  to tau nu decay channel in the fully hadronic final state at  $\sqrt{s} = 8$  TeV”, Technical Report CMS-PAS-HIG-14-020, CERN, 2014. Geneva, (Sep, 2014). See also [twiki.cern.ch/twiki/bin/view/CMSPublic/Hig14020Wiki](http://twiki.cern.ch/twiki/bin/view/CMSPublic/Hig14020Wiki).
- [9] ATLAS , “Search for charged Higgs bosons decaying via  $H^\pm \rightarrow \tau^\pm \nu$  in fully hadronic final states using pp collision data at  $\sqrt{s} = 8$  TeV with the ATLAS detector”, *JHEP* **1503** (2015) 088, doi:10.1007/JHEP03(2015)088, arXiv:1412.6663.
- [10] G. Degrandi, S. Heinemeyer, W. Hollik et al., “Towards high precision predictions for the MSSM Higgs sector”, *Eur.Phys.J.* **C28** (2003) 133–143, doi:10.1140/epjc/s2003-01152-2, arXiv:hep-ph/0212020.
- [11] B. Allanach, A. Djouadi, J. Kneur et al., “Precise determination of the neutral Higgs boson masses in the MSSM”, *JHEP* **0409** (2004) 044, doi:10.1088/1126-6708/2004/09/044, arXiv:hep-ph/0406166.
- [12] M. Carena, S. Heinemeyer, O. Stål et al., “MSSM Higgs Boson Searches at the LHC: Benchmark Scenarios after the Discovery of a Higgs-like Particle”, *Eur.Phys.J.* **C73** (2013), no. 9, 2552, doi:10.1140/epjc/s10052-013-2552-1, arXiv:1302.7033.
- [13] A. Arbey, M. Battaglia, and F. Mahmoudi, “Supersymmetric Heavy Higgs Bosons at the LHC”, *Phys.Rev.* **D88** (2013), no. 1, 015007, doi:10.1103/PhysRevD.88.015007, arXiv:1303.7450.
- [14] A. Djouadi and J. Quevillon, “The MSSM Higgs sector at a high  $M_{SUSY}$ : reopening the low  $\tan\beta$  regime and heavy Higgs searches”, *JHEP* **1310** (2013) 028, doi:10.1007/JHEP10(2013)028, arXiv:1304.1787.
- [15] G. Lee and C. E. M. Wagner, in preparation.
- [16] P. Draper, G. Lee, and C. E. M. Wagner, “Precise estimates of the Higgs mass in heavy supersymmetry”, *Phys.Rev.* **D89** (2014), no. 5, 055023, doi:10.1103/PhysRevD.89.055023, arXiv:1312.5743.
- [17] L. Maiani, A. Polosa, and V. Riquer, “Bounds to the Higgs Sector Masses in Minimal Supersymmetry from LHC Data”, *Phys.Lett.* **B724** (2013) 274–277, doi:10.1016/j.physletb.2013.06.026, arXiv:1305.2172.
- [18] A. Djouadi, L. Maiani, G. Moreau et al., “The post-Higgs MSSM scenario: Habemus MSSM?”, *Eur.Phys.J.* **C73** (2013) 2650, doi:10.1140/epjc/s10052-013-2650-0, arXiv:1307.5205.

- [19] A. Djouadi, L. Maiani, A. Polosa et al., “Fully covering the MSSM Higgs sector at the LHC”, *JHEP* **1506** (2015) 168, doi:10.1007/JHEP06(2015)168, arXiv:1502.05653.
- [20] S. Heinemeyer, in the web pages of the LHC-HXSWG-3: <https://twiki.cern.ch/twiki/pub/LHCPhysics/HXSWG3LowTanB/benchmark5-v0.pdf>.
- [21] S. Heinemeyer, W. Hollik, and G. Weiglein, “FeynHiggs: A Program for the calculation of the masses of the neutral CP even Higgs bosons in the MSSM”, *Comput.Phys.Commun.* **124** (2000) 76–89, doi:10.1016/S0010-4655(99)00364-1, arXiv:hep-ph/9812320.
- [22] S. Heinemeyer, W. Hollik, and G. Weiglein, “The Masses of the neutral CP - even Higgs bosons in the MSSM: Accurate analysis at the two loop level”, *Eur.Phys.J.* **C9** (1999) 343–366, doi:10.1007/s100529900006, arXiv:hep-ph/9812472.
- [23] M. Frank, T. Hahn, S. Heinemeyer et al., “The Higgs Boson Masses and Mixings of the Complex MSSM in the Feynman-Diagrammatic Approach”, *JHEP* **0702** (2007) 047, doi:10.1088/1126-6708/2007/02/047, arXiv:hep-ph/0611326.
- [24] T. Hahn, S. Heinemeyer, W. Hollik et al., “High-Precision Predictions for the Light CP -Even Higgs Boson Mass of the Minimal Supersymmetric Standard Model”, *Phys.Rev.Lett.* **112** (2014), no. 14, 141801, doi:10.1103/PhysRevLett.112.141801, arXiv:1312.4937.
- [25] LHC-HXSWG-3, <https://twiki.cern.ch/twiki/bin/view/LHCPhysics/LHCHXSWG3>.
- [26] A. Djouadi, J.-L. Kneur, and G. Moultaka, “SuSpect: A Fortran code for the supersymmetric and Higgs particle spectrum in the MSSM”, *Comput.Phys.Commun.* **176** (2007) 426–455, doi:10.1016/j.cpc.2006.11.009, arXiv:hep-ph/0211331.
- [27] R. V. Harlander, S. Liebler, and H. Mantler, “SusHi: A program for the calculation of Higgs production in gluon fusion and bottom-quark annihilation in the Standard Model and the MSSM”, *Comput.Phys.Commun.* **184** (2013) 1605–1617, doi:10.1016/j.cpc.2013.02.006, arXiv:1212.3249.
- [28] M. Spira, A. Djouadi, D. Graudenz et al., “Higgs boson production at the LHC”, *Nucl.Phys.* **B453** (1995) 17–82, doi:10.1016/0550-3213(95)00379-7, arXiv:hep-ph/9504378.
- [29] R. Harlander and P. Kant, “Higgs production and decay: Analytic results at next-to-leading order QCD”, *JHEP* **0512** (2005) 015, doi:10.1088/1126-6708/2005/12/015, arXiv:hep-ph/0509189.
- [30] R. V. Harlander and W. B. Kilgore, “Next-to-next-to-leading order Higgs production at hadron colliders”, *Phys.Rev.Lett.* **88** (2002) 201801, doi:10.1103/PhysRevLett.88.201801, arXiv:hep-ph/0201206.
- [31] R. V. Harlander and W. B. Kilgore, “Production of a pseudoscalar Higgs boson at hadron colliders at next-to-next-to leading order”, *JHEP* **0210** (2002) 017, doi:10.1088/1126-6708/2002/10/017, arXiv:hep-ph/0208096.
- [32] C. Anastasiou and K. Melnikov, “Higgs boson production at hadron colliders in NNLO QCD”, *Nucl.Phys.* **B646** (2002) 220–256, doi:10.1016/S0550-3213(02)00837-4, arXiv:hep-ph/0207004.

- [33] C. Anastasiou and K. Melnikov, “Pseudoscalar Higgs boson production at hadron colliders in NNLO QCD”, *Phys.Rev.* **D67** (2003) 037501, doi:10.1103/PhysRevD.67.037501, arXiv:hep-ph/0208115.
- [34] V. Ravindran, J. Smith, and W. L. van Neerven, “NNLO corrections to the total cross-section for Higgs boson production in hadron hadron collisions”, *Nucl.Phys.* **B665** (2003) 325–366, doi:10.1016/S0550-3213(03)00457-7, arXiv:hep-ph/0302135.
- [35] U. Aglietti, R. Bonciani, G. Degrossi et al., “Two loop light fermion contribution to Higgs production and decays”, *Phys.Lett.* **B595** (2004) 432–441, doi:10.1016/j.physletb.2004.06.063, arXiv:hep-ph/0404071.
- [36] R. Bonciani, G. Degrossi, and A. Vicini, “On the Generalized Harmonic Polylogarithms of One Complex Variable”, *Comput.Phys.Commun.* **182** (2011) 1253–1264, doi:10.1016/j.cpc.2011.02.011, arXiv:1007.1891.
- [37] R. V. Harlander and W. B. Kilgore, “Higgs boson production in bottom quark fusion at next-to-next-to leading order”, *Phys.Rev.* **D68** (2003) 013001, doi:10.1103/PhysRevD.68.013001, arXiv:hep-ph/0304035.
- [38] S. Dittmaier, M. Krämer, and M. Spira, “Higgs radiation off bottom quarks at the Tevatron and the CERN LHC”, *Phys.Rev.* **D70** (2004) 074010, doi:10.1103/PhysRevD.70.074010, arXiv:hep-ph/0309204.
- [39] S. Dawson, C. Jackson, L. Reina et al., “Exclusive Higgs boson production with bottom quarks at hadron colliders”, *Phys.Rev.* **D69** (2004) 074027, doi:10.1103/PhysRevD.69.074027, arXiv:hep-ph/0311067.
- [40] R. Harlander, M. Krämer, and M. Schumacher, “Bottom-quark associated Higgs-boson production: reconciling the four- and five-flavour scheme approach”, arXiv:1112.3478.
- [41] A. Martin, W. Stirling, R. Thorne et al., “Parton distributions for the LHC”, *Eur.Phys.J.* **C63** (2009) 189–285, doi:10.1140/epjc/s10052-009-1072-5, arXiv:0901.0002.
- [42] PDF4LHC, [http://www.hep.ucl.ac.uk/pdf4lh/PDF4LHC\\_practical\\_guide.pdf](http://www.hep.ucl.ac.uk/pdf4lh/PDF4LHC_practical_guide.pdf).
- [43] A. Djouadi, J. Kalinowski, and M. Spira, “HDECAY: A Program for Higgs boson decays in the standard model and its supersymmetric extension”, *Comput.Phys.Commun.* **108** (1998) 56–74, doi:10.1016/S0010-4655(97)00123-9, arXiv:hep-ph/9704448.
- [44] A. Djouadi, M. Mühlleitner, and M. Spira, “Decays of supersymmetric particles: The Program SUSY-HIT (SUSpect-SdecaY-Hdecay-InTerface)”, *Acta Phys.Polon.* **B38** (2007) 635–644, arXiv:hep-ph/0609292.
- [45] E. Braaten and J. Leveille, “Higgs Boson Decay and the Running Mass”, *Phys.Rev.* **D22** (1980) 715, doi:10.1103/PhysRevD.22.715.
- [46] N. Sakai, “Perturbative QCD Corrections to the Hadronic Decay Width of the Higgs Boson”, *Phys.Rev.* **D22** (1980) 2220, doi:10.1103/PhysRevD.22.2220.
- [47] T. Inami and T. Kubota, “Renormalization Group Estimate of the Hadronic Decay Width of the Higgs Boson”, *Nucl.Phys.* **B179** (1981) 171, doi:10.1016/0550-3213(81)90253-4.

- [48] M. Drees and K.-i. Hikasa, “Heavy Quark Thresholds in Higgs Physics”, *Phys.Rev.* **D41** (1990) 1547, doi:10.1103/PhysRevD.41.1547.
- [49] M. Drees and K.-i. Hikasa, “NOTE ON QCD CORRECTIONS TO HADRONIC HIGGS DECAY”, *Phys.Lett.* **B240** (1990) 455, doi:10.1016/0370-2693(90)91130-4.
- [50] S. Gorishnii, A. Kataev, S. Larin et al., “Corrected Three Loop QCD Correction to the Correlator of the Quark Scalar Currents and  $\gamma$  (Tot) ( $H^0 \rightarrow$  Hadrons)”, *Mod.Phys.Lett.* **A5** (1990) 2703–2712, doi:10.1142/S0217732390003152.
- [51] S. Gorishnii, A. Kataev, S. Larin et al., “Scheme dependence of the next to next-to-leading QCD corrections to Gamma(tot) ( $H^0 \rightarrow$  hadrons) and the spurious QCD infrared fixed point”, *Phys.Rev.* **D43** (1991) 1633–1640, doi:10.1103/PhysRevD.43.1633.
- [52] A. L. Kataev and V. T. Kim, “The Effects of the QCD corrections to Gamma ( $H^0 \rightarrow$  b anti-b)”, *Mod.Phys.Lett.* **A9** (1994) 1309–1326, doi:10.1142/S0217732394001131.
- [53] S. Gorishnii, A. Kataev, and S. Larin, “The Width of Higgs Boson Decay Into Hadrons: Three Loop Corrections of Strong Interactions”, *Sov.J.Nucl.Phys.* **40** (1984) 329–334.
- [54] L. R. Surguladze, “Quark mass effects in fermionic decays of the Higgs boson in O ( $\alpha$ -s\*\*2) perturbative QCD”, *Phys.Lett.* **B341** (1994) 60–72, doi:10.1016/0370-2693(94)01253-9, arXiv:hep-ph/9405325.
- [55] S. Larin, T. van Ritbergen, and J. Vermaseren, “The Large top quark mass expansion for Higgs boson decays into bottom quarks and into gluons”, *Phys.Lett.* **B362** (1995) 134–140, doi:10.1016/0370-2693(95)01192-S, arXiv:hep-ph/9506465.
- [56] K. Chetyrkin and A. Kwiatkowski, “Second order QCD corrections to scalar and pseudoscalar Higgs decays into massive bottom quarks”, *Nucl.Phys.* **B461** (1996) 3–18, doi:10.1016/0550-3213(95)00616-8, arXiv:hep-ph/9505358.
- [57] K. Chetyrkin, “Correlator of the quark scalar currents and Gamma(tot) ( $H \rightarrow$  hadrons) at O ( $\alpha$ -s\*\*3) in pQCD”, *Phys.Lett.* **B390** (1997) 309–317, doi:10.1016/S0370-2693(96)01368-8, arXiv:hep-ph/9608318.
- [58] P. Baikov, K. Chetyrkin, and J. H. Kuhn, “Scalar correlator at O( $\alpha$ (s)\*\*4), Higgs decay into b-quarks and bounds on the light quark masses”, *Phys.Rev.Lett.* **96** (2006) 012003, doi:10.1103/PhysRevLett.96.012003, arXiv:hep-ph/0511063.
- [59] LHC Higgs Cross Section Working Group, “Handbook of LHC Higgs Cross Sections: 3. Higgs Properties”, doi:10.5170/CERN-2013-004, arXiv:1307.1347.
- [60] A. Bredenstein, A. Denner, S. Dittmaier et al., “Precise predictions for the Higgs-boson decay  $H \rightarrow WW/ZZ \rightarrow 4$  leptons”, *Phys.Rev.* **D74** (2006) 013004, doi:10.1103/PhysRevD.74.013004, arXiv:hep-ph/0604011.
- [61] A. Bredenstein, A. Denner, S. Dittmaier et al., “Radiative corrections to the semileptonic and hadronic Higgs-boson decays  $H \rightarrow WW / ZZ \rightarrow 4$  fermions”, *JHEP* **0702** (2007) 080, doi:10.1088/1126-6708/2007/02/080, arXiv:hep-ph/0611234.
- [62] K. E. Williams, H. Rzehak, and G. Weiglein, “Higher order corrections to Higgs boson decays in the MSSM with complex parameters”, *Eur.Phys.J.* **C71** (2011) 1669, doi:10.1140/epjc/s10052-011-1669-3, arXiv:1103.1335.